ORIGINAL BASIC SCIENCE REPORT

OPEN

Longitudinal Validation of Right Ventricular Pressure Monitoring for the Assessment of Right Ventricular Systolic Dysfunction in a Large Animal Ischemic Model

Etienne J. Couture, MD[1]
Kevin Moses, MSc[2]
Manuel Ignacio Monge García, MD[3]
Cristhian Potes, PhD[2]
Francois Haddad, MD[4]
Lars Grønlykke, MD, PhD[5]
Fernando Garcia, ASc, BA[2]
Eden Paster, DVM[2]
Philippe Pibarot, DVM, PhD[6]
André Y. Denault, MD, PhD[7]

CONTEXT: Right ventricular (RV) dysfunction is a major cause of morbidity and mortality in intensive care and cardiac surgery. Early detection of RV dysfunction may be facilitated by continuous monitoring of RV waveform obtained from a pulmonary artery catheter. The objective is to evaluate the extent to which RV pressure monitoring can detect changes in RV systolic performance assess by RV end-systolic elastance (E_{es}) following the development of an acute RV ischemic in a porcine model.

HYPOTHESIS: RV pressure monitoring can detect changes in RV systolic performance assess by RV E_{es} following the development of an acute RV ischemic model.

METHODS AND MODELS: Acute ischemic RV dysfunction was induced by progressive embolization of microsphere in the right coronary artery to mimic RV dysfunction clinically experienced during cardiopulmonary bypass separation caused by air microemboli. RV hemodynamic performance was assessed using RV pressure waveform-derived parameters and RV E_{es} obtained using a conductance catheter during inferior vena cava occlusions.

RESULTS: Acute ischemia resulted in a significant reduction in RV E_{es} from 0.26 mm Hg/mL (interquartile range, 0.16–0.32 mm Hg/mL) to 0.14 mm Hg/mL (0.11–0.19 mm Hg/mL; $p < 0.010$), cardiac output from 6.3 L/min (5.7–7 L/min) to 4.5 (3.9–5.2 L/min; $p = 0.007$), mean systemic arterial pressure from 72 mm Hg (66–74 mm Hg) to 51 mm Hg (46–56 mm Hg; $p < 0.001$), and mixed venous oxygen saturation from 65% (57–72%) to 41% (35–45%; $p < 0.001$). Linear mixed-effect model analysis was used to assess the relationship between E_{es} and RV pressure-derived parameters. The reduction in RV E_{es} best correlated with a reduction in RV maximum first derivative of pressure during isovolumetric contraction (dP/dt_{max}) and single-beat RV E_{es}. Adjusting RV dP/dt_{max} for heart rate resulted in an improved surrogate of RV E_{es}.

INTERPRETATION AND CONCLUSIONS: Stepwise decreases in RV E_{es} during acute ischemic RV dysfunction were accurately tracked by RV dP/dt_{max} derived from the RV pressure waveform.

KEY WORDS: animal model; cardiac surgery; cardiogenic shock; pulmonary artery catheter; right ventricular function

Right ventricular (RV) dysfunction has been associated with increased morbidity and mortality in patients with heart failure (1), pulmonary hypertension, ischemic heart disease (2), and undergoing cardiac surgery (3–7). RV function is challenging to assess due to its geometry and contraction pattern. Three-dimensional echocardiography and cardiac magnetic resonance can provide a volumetric assessment of contractile function, while

DOI: 10.1097/CCE.0000000000000847

KEY POINTS

Question: The objective is to evaluate if right ventricular (RV) pressure monitoring can detect changes in RV systolic function assess by end-systolic elastance (E_{es}) in an acute ischemic model from selective microsphere embolization in right coronary artery.

Findings: In this animal model, induction of acute ischemia resulted in a significant reduction in RV E_{es} from 0.26 to 0.14 mm Hg/mL ($p < 0.010$). This reduction best correlated with a reduction in RV maximum first derivative of pressure during isovolumetric contraction (dP/dt_{max}) in a linear mixed-effect model.

Meaning: Continuous monitoring of RV dP/dt_{max} provide a reliable assessment of RV function that is closely related to E_{es}, which is the gold standard of RV systolic function evaluation.

right heart catheterization provide a pressure-based assessment. Measurements from these modalities are influenced by loading condition contrary to pressure-volume (PV) loop analysis obtained from conductance catheter that can generates load-independent parameters considered to be the gold standard to describe RV systolic function (8).

Continuous RV systolic function monitoring can be done using pulmonary artery catheter with an RV opening port (9, 10). Different iterations of this catheter have been introduced including models with RV port designed for insertion of a pacing wire (11, 12). Continuous RV pressure monitoring has emerged as a tool to continuously evaluate RV function during cardiac surgery (13). However, the clinical benefit of RV pressure monitoring compared with the traditional approach of using central venous pressure (CVP) and pulmonary artery pressure is not known (13, 14). Furthermore, it is not established which hemodynamic parameter derived from the pulmonary artery catheter correlates best with RV end-systolic elastance (E_{es}) in the context of acute RV systolic dysfunction (15).

A large animal model of RV myocardial ischemia induced by right coronary artery (RCA) microspheres embolization is proposed to evaluate the ability of RV pressure monitoring to track changes in RV systolic function. Microemboli caused by air or particles in the RCA due to suboptimal deairing maneuvers at the moment of cardiopulmonary bypass separation is known to be the culprit of acute RV dysfunction experienced during cardiac surgery (16). The two specific aims of this study are first, to create a progressive RV systolic dysfunction model assessed by RV E_{es} and second, to determine the association between hemodynamic parameters derived from RV pressure monitoring from pulmonary artery catheter and RV E_{es} obtained from the conductance catheter.

MATERIALS AND METHODS

Experiments and animal care were approved on January 28, 2019, by Edwards Lifescience's Institutional Animal Care and Use Committee at the Edwards Research Center (No. 2019-105: Identification of Swan-Ganz parameters for early detection/prediction of RV dysfunction/failure using a large porcine model). All procedures and housing were compliant with the U.S. Department of Agriculture Animal Welfare Act regulations and the Guide for the Care and Use of Laboratory Animals (Institute for Laboratory Animal Research, National Academies Press, Washington, DC, 2010, 8th Edition). The Animal Research: Reporting in Vivo Experiments 2.0 guidelines were used to elaborate this experiment (17).

Animal Preparation and Anesthesia

Ten Yorkshire crossbred female domestic pigs (*Sus scrofa domesticus*) with an age range of 4–5 months and a weight of 79–96 kg were premedicated with an intramuscular combination of telazol (4.4 mg/kg), ketamine (2.2 mg/kg), and xylazine (1.1 mg/kg). They were then orally intubated and mechanically ventilated using a FIO_2 of 0.5, tidal volume of 10 mL/kg, inspiratory to expiratory ratio of 1:2.5, and respiratory rate adjusted to maintain normocapnia. General anesthesia was maintained with 1–2% isoflurane and a mixture of oxygen, air and nitrous oxide without neuromuscular blocking agent. Fluid maintenance was provided intravenously by Ringer's lactate solution at 4 mL/kg/hr. Rectal temperature was monitored and kept between 37°C and 38°C using a heating pad. The adequacy of anesthesia was assessed every 15 minutes by inspecting the jaw tone and the toe pinch response. Animals

were killed at the end of the study with a lethal dose of sodium pentobarbital (90 mg/kg).

Acute Right Ventricular Dysfunction Model

The acute RV dysfunction was achieved by progressive microsphere embolization of the RCA (18). RCA catheterization was performed via left carotid artery with a SIM1 catheter (Cook, Bloomington, IN) using a standard technique with Amplatz Extra-Stiff wire (Cook) under fluoroscopy guidance. A mixed solution of 0.125 g Contour polyvinyl alcohol-microspheres (Boston Scientific, Marlborough, MA) of 45–150 μm of radius with 10 mL saline and 10 mL contrast were injected into the RCA in a 1 mL stepwise manner every 5 minutes.

Experimental Protocol

Each animal started at baseline hemodynamic value of mean arterial pressure (MAP) greater than 65 mm Hg, mixed venous oxygen saturation (Svo_2) greater than 60%, and stroke volume (SV) variation less than 10%. Otherwise, 500 mL of additional normal saline was given to optimize animal hemodynamics. Two baseline hemodynamic and PV loop measurements were taken with a 5-minute waiting period between each measurement followed by placement of the RCA catheter. After catheter placement was verified with fluoroscopy, microsphere injection for progressive RCA embolization began, with injections given every 5 minutes. After every three injections, the inferior vena cava (IVC) was occluded, and PV loops were recorded during apnea. Microspheres were injected in the RCA until reaching a cardiogenic shock defined by a 40% relative reduction of Svo_2 from the baseline. Histological RV examination were performed on two pigs (**Supplemental Fig. 1**, http://links.lww.com/CCX/B129).

Hemodynamic Monitoring

Instantaneous RV PV loop measurements were obtained from a 5–7F-lumen dual-field conductance catheter introduced through the right internal jugular vein with 12 equidistant electrodes and a high-fidelity pressure sensor (CA71083-PL; CD Leycom, Zoetermeer, The Netherlands) connected to a PV signal processor (Inca; CD Leycom). The catheter tip was positioned in the RV apex and the correct placement confirmed by fluoroscopy and the examination of the segmental RV PV loops. Any electrodes located outside the RV were excluded from analysis. RV PV data were acquired and analyzed by a dedicated software system (Conduct NT, Version 3.18.1; CD Leycom). The signals were recorded at 250 Hz and filtered using a 10 Hz low-pass filter. A pulmonary artery catheter (Swan-Ganz CCOmbo 777F8; Edwards Lifesciences, Irvine, CA) was introduced through the left internal jugular vein and used for continuous monitoring of CVP, Svo_2, SV, and cardiac output (CO) by intermittent thermodilution.

Continuous systemic pressure was measured in the right femoral artery. The femoral and pulmonary artery catheters were connected to a fluid-filled pressure transducer (TruWave DPT; Edwards Lifesciences), leveled with the heart, and zeroed at the beginning of the study. These fluid-filled derived pressure waveforms were transferred to a multiparametric monitor (Philips MP90, Latham, NY) and digitally stored into a dedicated software (ixTrend, Ixitos GmbH, Berlin, Germany) at a sampling rate of 125 Hz. The correct placement of all catheters was guided and verified by fluoroscopy. Blood gases, medications, and ventilator settings were manually recorded every hour. Continuous Svo_2 was calibrated in vitro at the beginning of the study and then validated every hour using the Svo_2 reported in blood gases.

Pressure-Volume Analysis

Volume signal calibration consisted of the determination of CO by the standard thermodilution method averaging the value of three to five thermodilutions of ice-cold saline boluses injected at the end of expiration. Correction for parallel conductance was performed by the hypertonic saline method (19, 20). The RV end-systolic PV relationship was determined from the analysis of the RV PV loops during a transient reduction in cardiac preload (**Fig. 1**). This was performed occluding the IVC using a 25 mm Fogarty balloon (Edwards Transfemoral Balloon Catheter, 9350BC25, Edwards Lifesciences) percutaneously introduced into the left femoral vein and advanced to the right atrial-IVC junction. The balloon was inflated with a syringe pump (PHD ULTRA, Harvard Apparatus, Holliston, MA) at a fixed rate, maintaining occlusion of the IVC for 5 seconds, and finally deflated to allow both pressure and volume to rapidly return to baseline.

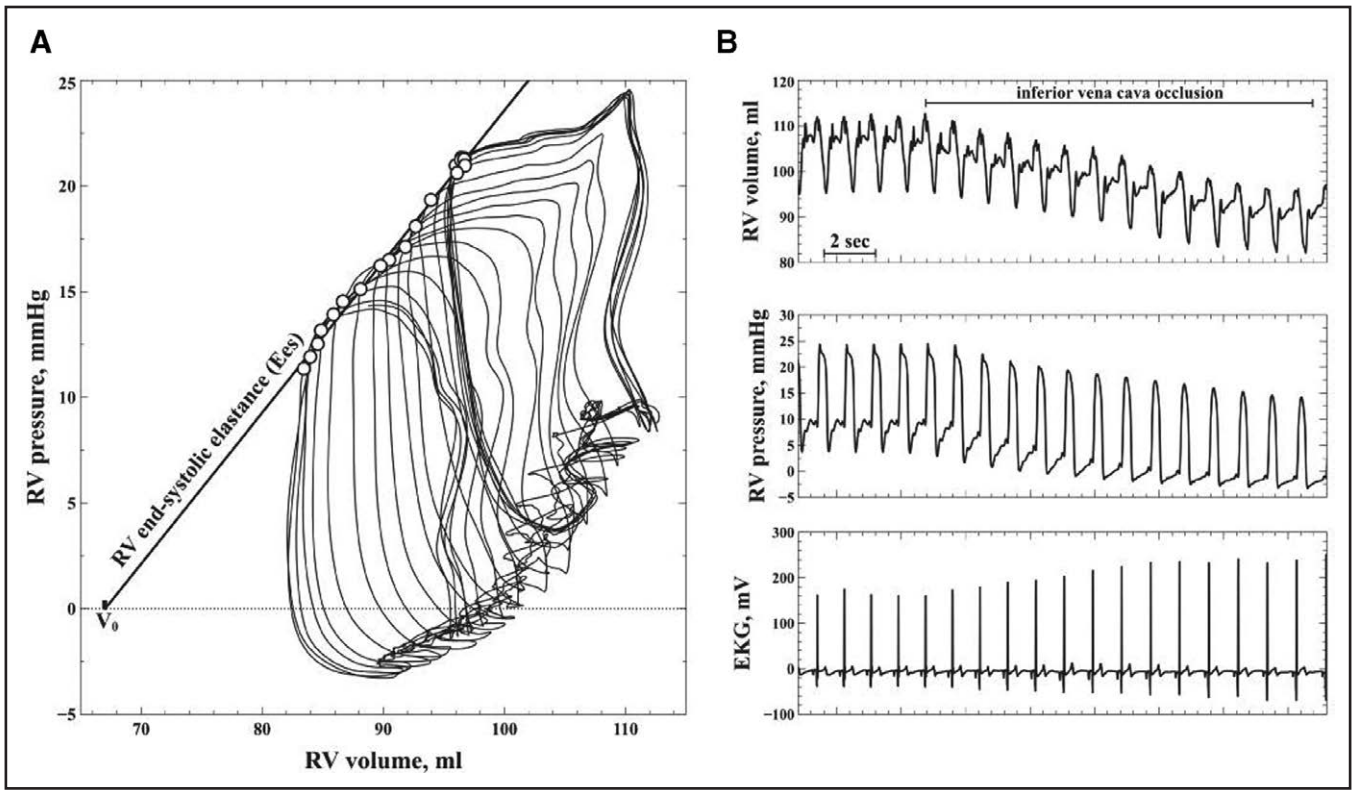

Figure 1. Example of the right ventricular (RV) pressure-volume analysis during an inferior vena cava occlusion. **A**, RV pressure-volume loops obtained during an inferior vena cava occlusion. **B**, Simultaneous recording of RV volume and RV pressure with electrocardiogram (ECG). *Open circles* in the pressure-volume loop are the maximal end-systolic elastance (E_{es}) for each cardiac cycle. The *slope* of end-systolic pressure-volume relationship obtained during a transient decrease in preload represents the RV E_{es}, a load-independent measure of RV contractility. The *point* where end-systolic pressure-volume relationship intersects the volume axis represents the RV unstressed volume (V_0), indicating the volume that the RV must fill before generating any pressure.

RV systolic function was characterized by the E_{es} from RV PV loop analysis during the IVC occlusion. E_{es} was calculated as the slope of the RV end-systolic PV relationship obtained from the linear regression analysis of the maximal elastance (E) points on each cardiac cycle (21), defined as $E(t) = P(t)/V(t)–V_0$, where V_0 is volume-axis intercept or the RV unstressed volume determined by the iterative method (Fig. 1) (22). E_{es} is considered a more load-independent measure of systolic function (23). The RV end-systolic pressure (ESP), RV end-diastolic volume (EDV), RV end-systolic volume (ESV), RV end-diastolic pressure (EDP), and RV ejection fraction (RVEF) were calculated from the conductance catheter taking the median value across a 5 to 10 seconds steady state during an end-expiratory apnea. End-systole was defined as the maximal PV ratio during each cardiac cycle and end-diastole was determined from the peak of the R wave on the electrocardiogram (22). Single-beat RV end-systolic elastance (E_{esSB}) is calculated from the ratio of RV ESP over RV ESV ratio. It does not require variation of loading conditions and neglects the RV V_0 (24, 25). Pulmonary effective arterial elastance ($E_{a\text{-}pulm}$) was used as a net measure of RV afterload, accounting for mean and pulsatile load, and calculated as the ratio of RV ESP over SV. Thermodilution technique from the pulmonary artery catheter was used to measure SV and CO.

Surrogates of Right Ventricular Systolic Function to Be Compared With Right Ventricular End-Systolic Elastance

Through progressive RV ischemia, the following parameters were assessed for relationship with RV E_{es}: a) the maximum first derivative of RV pressure during isovolumetric contraction (dP/dt_{max}) obtained from the RV pressure recording of both the conductance catheter and the pulmonary artery catheter; b) RV function index (RVFI) calculated as the ratio of RV ESP over CO obtained from pulmonary artery catheter (26); c)

stroke work (SW), calculated from the area within the PV loop; d) RVEF calculated from the SV and EDV obtained from the conductance catheter and; e) RV E_{esSB} obtained from conductance catheter.

Statistical Analysis

Sample size was calculated for detecting a mean RV E_{es} difference of 0.25 mm Hg/mL (SD 0.25 mm Hg/mL) between baseline and end-stage RV dysfunction, with an 80% of power and error α of 0.05. Quantitative data are expressed as median and interquartile range except when specified. Quantitative data were compared using nonparametric Mann-Whitney rank tests for unpaired data and Wilcoxon matched-pairs signed rank test for paired data. A linear mixed-effects model analysis was used for assessing the relationship between continuous variables, using individual animals as a subject for random factors and sequential experimental stages as repeated measurements. Specifically, the analysis used a random intercept component to account for any individual differences in the intercept between pigs (27). Reported parameters include the estimated coefficient as well as the 95% CI for the coefficient, *z* score, and *p* value. *p* values of less than 0.05 were considered significant. All analyses were implemented in Python (Python Software Foundation, Beaverton, OR, Python Language Reference, Version 3.7, available at https://www.python.org) with StatsModel library.

RESULTS

Progressive RV dysfunction was induced until obtaining end-stage RV dysfunction. The gross examination of hearts submitted to histological study confirmed microscopic features of ischemia with the presence of wavy fibers (Supplemental Fig. 1, http://links.lww.com/CCX/B129). Change in RV systolic function was characterized by a gradual reduction through microsphere injections process, resulting in an overall 50% decrease in E_{es} from baseline to end-stage RV dysfunction (from 0.26 to 0.14 mm Hg/mL; $p = 0.0102$) (**Supplemental Fig. 2**, http://links.lww.com/CCX/B129). End-stage RV dysfunction was associated with a cardiogenic shock condition with a significant reduction in systemic MAP (from 72 to 51 mm Hg; $p = 0.0002$), Svo_2 (from 65% to 41%; $p = 0.0006$), and CO (from 6.3 to 4.5 L/min; $p = 0.0074$) (**Table 1**). Changes in CVP (from 6 to 9 mm Hg; $p = 0.0601$) and RV EDP (from 8 to 10 mm Hg; $p = 0.0696$) were not statistically significant from baseline to end-stage RV dysfunction. Morphological changes in the PV loops through the progression of RV dysfunction were characterized by a gradual shift of the loop to larger volume values and smaller intraventricular pressure gradient due to a lower RV ESP and higher RV EDP. This phenomenon resulted in a significant reduction in SW (**Supplemental Fig. 3**, http://links.lww.com/CCX/B129).

All prespecified surrogates of RV systolic function and E_{es} were significantly reduced by RV dysfunction except for RVEF (**Fig. 2**). To determine the best variable associated with changes in RV E_{es}, a univariate linear mixed model was performed using RV surrogates as covariates (fixed effects) and RV E_{es} as the dependent variable. All systolic function surrogates were significantly related to E_{es}; RV dP/dt_{max} was the best estimate according to the *z* score followed by the single-beat E_{esSB} (**Table 2**). For each increase in 1 mm Hg/s of RV dP/dt_{max}, RV E_{es} increased 1.185×10^{-3} mm Hg/mL (95% CI, 0.957–1.413, *z* score = 10.18; $p < 0.001$).

A multivariate mixed model regression analysis was used to evaluate the contribution of other parameters on RV dP/dt_{max}. Heart rate, RV EDV, EDP, ESV and $E_{a\text{-}pulm}$ were used as fixed effects and RV dP/dt_{max} as the dependent variable. RV dP/dt_{max} was positively related to heart rate, RV E_{es}, EDV, and $E_{a\text{-}pulm}$, and negatively associated to RV ESV and EDP (**Table 3**). Further analysis was performed in which RV dP/dt_{max} was normalized by these parameters and then used in the univariate linear mixed model analysis described above (**Supplemental Table 1**, http://links.lww.com/CCX/B129). Using this analysis, the ratio of RV dP/dt_{max} over heart rate resulted in a better surrogate of E_{es} than RV dP/dt_{max} alone according to the lower Akaike information criterion. Finally, both RV dP/dt_{max} obtained from conductance catheter and the pulmonary artery catheter with dedicated RV port demonstrated similar relation with RV E_{es} (**Table 4**).

DISCUSSION

The main findings of the study are three-fold. First, a stepwise change in RV systolic function was observed using an animal model of acute and progressive RV ischemic cardiogenic shock induced by RCA microsphere

TABLE 1.
Main Hemodynamic Variables Comparison Before and After Inducing Right Ventricular Failure

Variable	Baseline	End-Stage RV Dysfunction	*p*[a]	Difference (95% CI)[b]
Heart rate, beats/min	73 (70–74)	86 (65–101)	0.3447	19 (–8 to 32)
Systemic mean arterial pressure, mm Hg	72 (66–74)	51 (46–56)	0.0002	–20 (–29 to –14)
Mixed venous oxygen saturation, %	65 (57–72)	41 (35–45)	0.0006	–23 (–34 to –16)
Hemodynamic parameter issued from the conductance catheter				
RV end-systolic volume, mL	144 (89–176)	199 (144–247)	0.1124	61 (–11 to 122)
RV end-diastolic volume, mL	231 (180–254)	277 (238–329)	0.1306	43 (–13 to 114)
RV stroke volume, mL	88 (80–96)	78 (63–95)	0.3258	–11 (–27 to 8)
RV ESP, mm Hg	19 (18–21)	14 (11–18)	0.0233	–4 (–8 to –1)
RV end-diastolic pressure, mm Hg	8 (6–9)	10 (8–11)	0.0696	2 (0–4)
RV ejection fraction, %	41 (29–53)	30 (26–36)	0.1736	–9 (–26 to 3)
Maximum RV pressure rise during isovolumetric contraction, mm Hg/s	238 (191–295)	162 (133–177)	0.0082	–71 (–132 to –26)
Stroke work, mmHg/mL	1,457 (1,264–1,653)	928 (793–1,028)	0.0032	–500 (–808 to –243)
RV end-systolic elastance, mm Hg/mL	0.26 (0.16–0.32)	0.14 (0.11–0.19)	0.0102	–0.08 (–0.22 to –0.02)
RV single-beat end-systolic elastance, mm Hg/mL	0.19 (0.09–0.25)	0.08 (0.06–0.10)	0.0102	–0.05 (–0.22 to –0.02)
Pulmonary arterial effective elastance, mm Hg/mL	0.23 (0.21–0.26)	0.20 (0.13–0.26)	0.4963	–0.04 (–0.11 to 0.05)
Hemodynamic parameter issued from the pulmonary artery catheter				
Central venous pressure, mm Hg	6 (6–7)	9 (8–10)	0.0601	2 (0–6)
RV systolic pressure, mm Hg	24 (22–28)	20 (17–21)	0.0191	–5 (–8 to –1)
Systolic PAP, mm Hg	25 (24–26)	21 (21–22)	0.0136	–4 (–7 to –1)
Diastolic PAP, mm Hg	16 (14–18)	14 (12–14)	0.0142	–2 (–6 to 2)
Mean PAP, mm Hg	20 (18–21)	17 (15–18)	0.0452	–3 (–6 to 0)
CO, L/min	6.3 (5.7–7.0)	4.5 (3.9–5.2)	0.0074	–1.9 (–3.1 to –0.6)
Stroke volume, mL	78 (71–89)	48 (39–57)	0.0104	–31 (–49 to –12)
RV function index (RV ESP/CO), mmHg/min/L	3.99 (3.62–4.44)	3.17 (2.71–3.60)	0.0283	–0.74(–1.64 to –0.09)
Arterial blood gas				
pH	7.59 (7.56–7.63)	7.54 (7.50–7.57)	0.0640	–0.05 (–0.10 to 0.00)
$Paco_2$, mm Hg	33 (29–37)	34 (30–39)	0.4057	2 (–4 to 8)
Pao_2, mm Hg	197 (162–227)	144 (118–177)	0.0696	–55 (–110 to 1)
Hco_3^-, mmol/L	32 (31–33)	29 (27–31)	0.0494	–3 (–5 to 0)
Lactates, mmol/L	2.0 (1.8–2.3)	2.4 (2.2–2.5)	0.0257	0.5 (0.1–0,8)
Hemoglobin, g/dL	9.9 (9.4–10.4)	9.5 (8.4–10.4)	0.3075	–0.6 (–1.7 to 0.5)

CO = cardiac output, ESP = end-systolic pressure, Hco3 = icarbonate, PAP = pulmonary artery pressure, RV = right ventricle.

[a]Wilcoxon test comparison.

[b]Median difference based on the Hodges-Lehmann method (95% CI).

Values are expressed as median (25–75th interquartile range), except where otherwise stated.

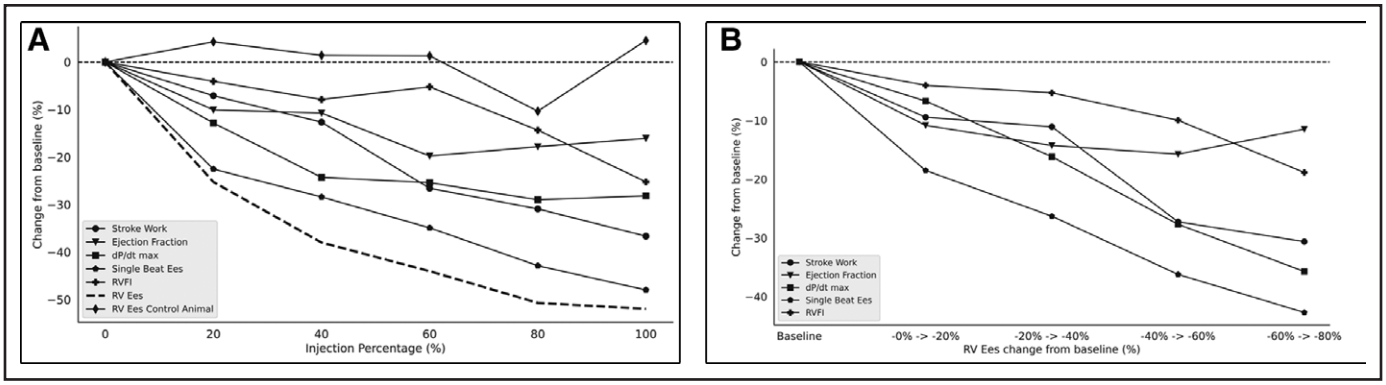

Figure 2. Assessment of right ventricular (RV) systolic function in acute progressive RV dysfunction model. **A**, Progressive change from baseline (%) in RV end-systolic elastance (E_{es}) and surrogates of RV function explored during the progressive embolization of the right coronary artery by microspheres injections. A control animal submitted to placebo (saline) injection in the right coronary artery instead of microsphere did not show significant variation in RV E_{es}. Microsphere injections are presented as percentage of total injection per subject, 0 being the baseline and 100% being final injections. **B**, Progressive change from baseline (%) of surrogates of RV function according to changes in RV E_{es} during the progressive embolization of the right coronary artery by microspheres injections. dP/dt_{max} = maximum first derivative of pressure during isovolumetric contraction, RVFI = right ventricular function index.

TABLE 2.
Linear Mixed Model Analysis of the Relationship Between Right Ventricular End-Systolic Elastance and Systolic Function Surrogates

Fixed Effects	Estimated Coefficient	End-Systolic Elastance Scaling Factor	*z*	*p* > |*z*|	95% CI
Maximum RV pressure rise during isovolumetric contraction, mm Hg/s	1.185	1,000	10.184	< 0.001	0.957–1.413
Single-beat end-systolic elastance, mm Hg/mL	0.734	1	9.916	< 0.001	0.589–0.879
Stroke work, mmHg/mL	0.137	1,000	7.475	< 0.001	0.101–0.173
RV ejection fraction, %	5.052	1,000	7.12	< 0.001	3.662–6.443
RV function index (RV end-systolic pressure/cardiac output), mmHg/min/L	32.756	1,000	3.016	0.003	11.471–54.041

RV = right ventricular.

Estimates reflect the average change in end-systolic elastance (E_{es}) × E_{es} scaling factor per unit increase of the fixed effect except for single-beat end-systolic elastance.

embolization allowing longitudinal hemodynamic analysis of systolic function. Second, pulmonary artery catheter-derived RV dP/dt_{max} was related to progressive changes in RV E_{es}. Third, improvement of the correlation of pulmonary artery catheter-derived RV dP/dt_{max} with RV E_{es} can be obtained by normalizing it by heart rate.

The presented study was performed to validate, in an animal model, clinical observations made related to the use of continuous RV pressure monitoring during cardiac surgery. In fact, continuous RV pressure monitoring during cardiac surgery was initially introduced to diagnose RV outflow tract obstruction (RVOTO) (28). Severe RVOTO can lead to a shock state called "suicide RV," which is fatal if unrecognized (29–31). As experience grew with the use of RV pressure waveform, it became apparent that this monitoring could be used to diagnose severe RV dysfunction with reduced RV dP/dt_{max} following coronary artery air embolism in the operating room and in the ICU (16, 32–34). The objective of this study was to determine the association between hemodynamic parameters derived from RV pressure monitoring and RV E_{es} obtained from the conductance catheter, which

TABLE 3.
Mixed Linear Model Regression Analysis of the Relationship Between Right Ventricular Maximum First Derivative of Pressure During Isovolumetric Contraction and Right Ventricular Parameters

Fixed Effects	Estimated Coefficient	*z*	*p* > |*z*|	95% CI
End-systolic elastance, mm Hg/mL	195.317	5.806	< 0.001	129.379–261.254
Pulmonary effective arterial elastance, mm Hg/mL	597.925	6.746	< 0.001	424.209–771.641
Heart rate, beats/min	2.26	8.44	< 0.001	1.735–2.785
RV end-diastolic pressure, mm Hg	−8.727	−4.368	< 0.001	−12.643 to −4.812
RV end-diastolic volume, mL	2.342	6.809	< 0.001	1.668–3.016
RV end-systolic volume, mL	−2.664	−8.331	< 0.001	−3.291 to −2.037

RV = right ventricular.
Estimates reflect the average change in maximum RV pressure rise during isovolumetric contraction per unit increase of the fixed effect.

TABLE 4.
Linear Mixed Model Analysis of the Relationship Between Right Ventricular End-Systolic Elastance and Maximum Right Ventricular Pressure Rise During Isovolumetric Contraction Derived From Conductance and Fluid-Filled Catheter

Fixed Effects	Estimated Coefficient	*z*	*p* > |*z*|	95% CI	R^2
From conductance catheter: RV dP/dt_{max}, mm Hg/s	1.12	10.883	< 0.001	0.919–1.322	0.7273
From fluid-filled pulmonary artery catheter: RV dP/dt_{max}, mm Hg/s	0.73	7.716	< 0.001	0.544–0.915	0.634

RV dP/dt_{max} = maximum right ventricular pressure rise during isovolumetric contraction.
Estimates reflect the average change in right ventricular end-systolic elastance per unit of RV dP/dt_{max}.

represents the gold standard method of RV systolic performance assessment (8). Identification of variables derived from the RV pressure waveform associated with changes in RV E_{es} would precociously inform on the early and progressive appearance RV systolic dysfunction. Clinically, early identification of RV systolic dysfunction using continuous RV pressure monitoring would help to trigger proper management using inotropes and pulmonary vasodilators to reverse and mitigate progression of RV systolic dysfunction to RV failure and systemic complication.

Pulmonary artery catheter equipped with a RV opening can provide continuous hemodynamic monitoring of the right atrial, pulmonary artery and RV pressures, in addition to SV, CO, and Svo_2. While echocardiographic assessment of the RV relies on a proper acoustic window and provides intermittent information, pulmonary artery catheterization using such catheter is continuous and feasible in 93.5% of the patients undergoing cardiac surgery (13, 14). Results from this animal study shows that conventional hemodynamic parameter such as CVP, usually tracked as a surrogate of RV performance in the absence of pulmonary artery catheter, is not affected even by a 50% decrease in RV E_{es}, whereas parameters obtained from RV pressure monitoring such as RV dP/dt_{max} is more sensitive and change earlier in the process of RV acute ischemic injury. This highlights the benefit of using a pulmonary catheter in situations with risk of RV dysfunction such as during cardiac surgery.

Optimally, a hemodynamic parameter to evaluate RV systolic function should primarily be influenced by contractility and unaffected by loading conditions.

E_{es} obtained by a conductance catheter during a transient preload reduction is a load-independent index of ventricular contractility (8, 19, 35). However, this technique is not clinically feasible due to the invasiveness, risk of complications and sophisticated computational analysis required. Thus, to find an optimal parameter to track RV systolic function in acute care setting, parameters derived from the RV pressure and volume monitoring were tested. Among the chosen RV systolic function variables, RV pressure monitoring allows calculating dP/dt_{max}, RVFI, and SW, while E_{esSB} and RVEF can only be obtained by incorporating simultaneous volumetric assessment. When looking at the prespecified surrogates of RV systolic function, all of them showed significant relationship with RV E_{es} through various levels of systolic function, with RV dP/dt_{max} showing the best association.

Evaluation of RV systolic function by dP/dt_{max} obtained from RV pressure monitoring using right heart catheterization or conductance catheter have been previously described (36). This parameter is known to be influenced by loading conditions (37, 38). According to the presented model, RV dP/dt_{max} was influenced by E_{es} and $E_{a\text{-}pulm}$, which is consistent with previous findings (38). Increased preload is a known stimulus for enhancing systolic function by raising the rate of isovolumetric contraction, which manifests by an increased RV dP/dt_{max}, especially in patients without RV dysfunction (37, 38). Variations in RV EDP and EDV in the presented model were associated with changes in RV dP/dt_{max} consistent with previously reported observations (39). Changes in heart rate associated with a reduction in contractility may mask changes in dP/dt_{max} (40). Thus, it is difficult to assess the effect of a condition that induces simultaneous changes in inotropism and chronotropism (39). Given the significant association of heart rate with dP/dt_{max}, an adjustment was applied dividing dP/dt_{max} by heart rate providing a better fit to RV E_{es} (Supplemental Table 1, http://links.lww.com/CCX/B129).

Various techniques using the single-beat method have been used to assess RV E_{es} (41–43). Despite their potential usefulness, these methods use the relatively short-lived isovolumetric periods to estimate the maximal rise in pressure in order to calculate E_{esSB} (44). However, the brief duration of these periods in RV compared with left ventricle accentuate the risk for errors. RV volume monitoring from conductance catheter has also limitations due to the irregular PV loop morphology with progression of RV dysfunction. This was the primary reason that supported the use of thermodilution to monitor SV. Regardless of these limitations, significant reduction in E_{esSB} from baseline to end-stage RV dysfunction was consistent with RV E_{es} variations. Among the chosen surrogates of RV systolic function, RVFI and RVEF may be more considered as right ventriculo-arterial coupling parameters. The other prespecified surrogates, $dP/dt_{max,}$ E_{esSB}, and SW, showed the highest association with changes in RV E_{es} highlighting their representativity of systolic function despite being dependent of loading conditions.

The presented animal model of RV dysfunction is staged, meaning RV systolic function was assessed from baseline to end-stage dysfunction to evaluate the parameters issued from the RV pressure monitoring that could act as surrogate of E_{es}. $E_{a\text{-}pulm}$ was unchanged through the protocol, indicating that the global reduction in RV systolic function was primarily due to a deficit in inotropism and not an acute increase in afterload. Previous animal models of RV dysfunction have been done using RCA ligation or embolization; however, they did not evaluate RV systolic function at different levels of dysfunction (45, 46).

The induction of RV dysfunction was achieved in animals under general anesthesia and mechanical ventilation, which are known factors that may affect RV function. The experimental protocol has been tested on a control animal with saline injection in the RCA, and it did not show significant variation in RV E_{es} (**Fig. 2*A***). The actual model preserves the chest intact and the interaction between the intrathoracic pressures and the heart, which overcomes many of the limitations of open-chest models. Despite these precautions, translation to human physiology should be done cautiously. The presented study focused on acute effects of myocardial ischemia on RV systolic dysfunction and might not be applicable to other mechanisms such as afterload increase. We are currently finalizing two studies in cardiac patients where continuous RV pressure waveform parameters will be evaluated (NCT04092855 and NCT04782154). Those will help in determining how sensitive changes in dP/dt are in detecting abnormal RV dysfunction. We have, however, reported that increases in dP/dt were clearly associated with improvement in RV function (32, 47, 48)

CONCLUSIONS

Stepwise changes in RV E_{es} were obtained secondary to progressive RV ischemic dysfunction up to cardiogenic shock induced by RCA microsphere embolization. RV dP/dt_{max} derived from the pulmonary artery catheter was found to be the most predictive surrogate of the reduction in E_{es}. These findings support the use of continuous RV pressure monitoring obtained from the pulmonary artery catheter as a sensitive monitor of RV systolic function. Continuous monitoring of the RV dP/dt_{max} could provide an opportunity for early initiation of treatment of RV dysfunction in order to mitigate its progression to severe form.

1 *Department of Anesthesiology & Division of Intensive Care Medicine, Institut Universitaire de Cardiologie et de Pneumologie de Québec, Québec, QC, Canada.*

2 *Edwards Lifesciences, Irvine, CA.*

3 *Department of Intensive Care Medicine, Hospital Universitario SAS de Jerez, Jerez de la Frontera, Spain.*

4 *Department of Cardiovascular Medicine, Stanford University, Stanford, CA.*

5 *Department of Cardiothoracic Anaesthesiology, Copenhagen University Hospital, Copenhagen, Denmark.*

6 *Research Center, Institut Universitaire de Cardiologie et de Pneumologie de Québec, Québec, QC, Canada.*

7 *Department of Anesthesiology & Division of Intensive Care Medicine, Montreal Heart Institute, Université de Montréal, Montreal, QC, Canada.*

Supplemental digital content is available for this article. Direct URL citations appear in the printed text and are provided in the HTML and PDF versions of this article on the journal's website (http://journals.lww.com/ccejournal).

Dr. Couture, Mr. Moses, Dr. Potes, Dr. Grønlykke, and Dr. Denault were involved in contribution to conception and design, acquisition of data, analysis and interpretation of data, drafting the article and revising it critically for important intellectual content. Drs. Monge Garcia and Haddad were involved in contribution to conception and design, analysis and interpretation of data, drafting the article and revising it critically for important intellectual content. Mr. Garcia and Dr. Paster were involved in contribution to conception and design, acquisition of data, and revising the article critically for important intellectual content. Dr. Pibarot was involved in analysis and interpretation of data, and revising the article critically for important intellectual content. All authors gave final approval of the version to be published and are in agreement to be accountable for all aspects of the work in ensuring that questions related to the accuracy or integrity of any part of the work are appropriately investigated and resolved.

This work was supported by Edwards, the Montreal Heart Institute Foundation, and the Richard Kaufman Endowment Fund in Anesthesia and Critical Care.

Mr. Moses, Dr. Potes, Mr. Garcia, and Dr. Paster work for Edwards Lifesciences—a manufacturer of healthcare devices and critical care solutions. Dr. Denault is on the speaker's bureau for CAE Healthcare (2012), Masimo (2017) and received an equipment grant from Edwards (2019). He is a consultant for Masimo (2020) and CAE Healthcare (2020). Dr. Monge García is a consultant for Edwards Lifesciences and Dextera Medical. The remaining authors have disclosed that they do not have any potential conflicts of interest.

For information regarding this article, E-mail: andre.denault@umontreal.ca

REFERENCES

1. Ghio S, Gavazzi A, Campana C, et al: Independent and additive prognostic value of right ventricular systolic function and pulmonary artery pressure in patients with chronic heart failure. *J Am Coll Cardiol* 2001; 37:183–188
2. Anavekar NS, Skali H, Bourgoun M, et al: Usefulness of right ventricular fractional area change to predict death, heart failure, and stroke following myocardial infarction (from the VALIANT ECHO study). *Am J Cardiol* 2008; 101:607–612
3. Maslow AD, Regan MM, Panzica P, et al: Precardiopulmonary bypass right ventricular function is associated with poor outcome after coronary artery bypass grafting in patients with severe left ventricular systolic dysfunction. *Anesth Analg* 2002; 95:1507–1518
4. Haddad F, Couture P, Tousignant C, et al: The right ventricle in cardiac surgery, a perioperative perspective: II. Pathophysiology, clinical importance, and management. *Anesth Analg* 2009; 108:422–433
5. Kormos RL, Teuteberg JJ, Pagani FD, et al: Right ventricular failure in patients with the HeartMate II continuous-flow left ventricular assist device: Incidence, risk factors, and effect on outcomes. *J Thorac Cardiovasc Surg* 2010; 139:1316–1324
6. Denault AY, Pearl RG, Michler RE, et al: Tezosentan and right ventricular failure in patients with pulmonary hypertension undergoing cardiac surgery: The TACTICS trial. *J Cardiothorac Vasc Anesth* 2013; 27:1212–1217
7. Denault AY, Bussieres JS, Arellano R, et al: A multicentre randomized-controlled trial of inhaled milrinone in high-risk cardiac surgical patients. *Can J Anesth* 2016; 63:1140–1153
8. Brener MI, Masoumi A, Ng VG, et al: Invasive right ventricular pressure-volume analysis: Basic principles, clinical applications, and practical recommendations. *Circ Heart Fail* 2022; 15:e009101
9. Saxena A, Garan AR, Kapur NK, et al: Value of hemodynamic monitoring in patients with cardiogenic shock undergoing mechanical circulatory support. *Circulation* 2020; 141:1184–1197
10. Garan AR, Kanwar M, Thayer KL, et al: Complete hemodynamic profiling with pulmonary artery catheters in cardiogenic shock is associated with lower in-hospital mortality. *JACC Heart Fail* 2020; 8:903–913
11. Bootsma IT, Boerma EC, de Lange F, et al: The contemporary pulmonary artery catheter. Part 1: Placement and waveform analysis. *J Clin Monit Comput* 2022; 36:5–15
12. Bootsma IT, Boerma EC, Scheeren TWL, et al: The contemporary pulmonary artery catheter. Part 2: Measurements,

limitations, and clinical applications. *J Clin Monit Comput* 2022; 36:17–31

13. Raymond M, Gronlykke L, Couture EJ, et al: Perioperative right ventricular pressure monitoring in cardiac surgery. *J Cardiothorac Vasc Anesth* 2019; 33:1090–1104
14. Gronlykke L, Couture EJ, Haddad F, et al: Preliminary experience using diastolic right ventricular pressure gradient monitoring in cardiac surgery. *J Cardiothorac Vasc Anesth* 2020; 34:2116–2125
15. Lahm T, Douglas IS, Archer SL, et al; American Thoracic Society Assembly on Pulmonary Circulation: Assessment of right ventricular function in the research setting: Knowledge gaps and pathways forward. An official American Thoracic Society Research Statement. *Am J Respir Crit Care Med* 2018; 198:e15–e43
16. Denault A, Haddad F, Lamarche Y, et al: Commentary: Postoperative right ventricular dysfunction-integrating right heart profiles beyond long-axis function. *J Thorac Cardiovasc Surg* 2020; 159:e315–e317
17. Percie du Sert N, Ahluwalia A, Alam S, et al: Reporting animal research: Explanation and elaboration for the ARRIVE guidelines 2.0. *PLoS Biol* 2020; 18:e3000411
18. Moller-Helgestad OK, Ravn HB, Moller JE: Large porcine model of profound acute ischemic cardiogenic shock. *Methods Mol Biol* 2018; 1816:343–352
19. Kass DA, Yamazaki T, Burkhoff D, et al: Determination of left ventricular end-systolic pressure-volume relationships by the conductance (volume) catheter technique. *Circulation* 1986; 73:586–595
20. Baan J, van der Velde ET, de Bruin HG, et al: Continuous measurement of left ventricular volume in animals and humans by conductance catheter. *Circulation* 1984; 70:812–823
21. Kass DA, Midei M, Graves W, et al: Use of a conductance (volume) catheter and transient inferior vena caval occlusion for rapid determination of pressure-volume relationships in man. *Cathet Cardiovasc Diagn* 1988; 15:192–202
22. Kono A, Maughan WL, Sunagawa K, et al: The use of left ventricular end-ejection pressure and peak pressure in the estimation of the end-systolic pressure-volume relationship. *Circulation* 1984; 70:1057–1065
23. Kass DA, Maughan WL: From "Emax" to pressure-volume relations: A broader view. *Circulation* 1988; 77:1203–1212
24. Sanz J, Garcia-Alvarez A, Fernandez-Friera L, et al: Right ventriculo-arterial coupling in pulmonary hypertension: A magnetic resonance study. *Heart* 2012; 98:238–243
25. Mehmood M, Biederman RWW, Markert RJ, et al: Right heart function in critically ill patients at risk for acute right heart failure: A description of right ventricular-pulmonary arterial coupling, ejection fraction and pulmonary artery pulsatility index. *Heart Lung Circ* 2020; 29:867–873
26. Saydain G, Awan A, Manickam P, et al: Pulmonary hypertension an independent risk factor for death in intensive care unit: Correlation of hemodynamic factors with mortality. *Clin Med Insights Circ Respir Pulm Med* 2015; 9:27–33
27. Fitzmaurice GM, Laird NM, Ware JH: Modeling the covariance. In: *Applied Longitudinal Analysis*. John Wiley & Sons, Inc. Second Edition. Hoboken, NJ, Wiley, 2011, pp 165–188
28. Denault AY, Chaput M, Couture P, et al: Dynamic right ventricular outflow tract obstruction in cardiac surgery. *J Thorac Cardiovasc Surg* 2006; 132:43–49
29. Kroshus TJ, Kshettry VR, Hertz MI, et al: Suicide right ventricle after lung transplantation for Eisenmenger syndrome. *Ann Thorac Surg* 1995; 59:995–997
30. Singhal A, Kumar S, Kapoor A: Sudden iatrogenic suicidal right ventricle. *Indian Heart J* 2015; 67:406–408
31. Gangahanumaiah S, Scarr BC, Buckland MR, et al: Suicide right ventricle after lung transplantation for pulmonary vascular disease. *J Card Surg* 2018; 33:412–415
32. Zeng YH, Calderone A, Beaubien-Souligny W, et al: Right ventricular outflow tract obstruction in the intensive care unit: A case report of 2 patients. *A A Pract* 2021; 15:e01532
33. Denault A, Lamarche Y, Rochon A, et al: Innovative approaches in the perioperative care of the cardiac surgical patient in the operating room and intensive care unit. *Can J Cardiol* 2014; 30:S459–S477
34. Hrymak C, Strumpher J, Jacobsohn E: Acute right ventricle failure in the intensive care unit: Assessment and management. *Can J Cardiol* 2017; 33:61–71
35. Burkhoff D, Mirsky I, Suga H: Assessment of systolic and diastolic ventricular properties via pressure-volume analysis: A guide for clinical, translational, and basic researchers. *Am J Physiol Heart Circ Physiol* 2005; 289:H501–H512
36. McCabe C, White PA, Rana BS, et al: Right ventricle functional assessment: Have new techniques supplanted the old faithful conductance catheter? *Cardiol Rev* 2014; 22:233–240
37. Quinones MA, Gaasch WH, Alexander JK: Influence of acute changes in preload, afterload, contractile state and heart rate on ejection and isovolumic indices of myocardial contractility in man. *Circulation* 1976; 53:293–302
38. Stein PD, Sabbah HN, Anbe DT, et al: Performance of the failing and nonfailing right ventricle of patients with pulmonary hypertension. *Am J Cardiol* 1979; 44:1050–1055
39. Mason DT: Usefulness and limitations of the rate of rise of intraventricular pressure (dp-dt) in the evaluation of myocardial contractility in man. *Am J Cardiol* 1969; 23:516–527
40. Bennett T, Sharma A, Sutton R, et al: Development of a rate adaptive pacemaker based on the maximum rate-of-rise of right ventricular pressure (RV dP/dtmax). *Pacing Clin Electrophysiol* 1992; 15:219–234
41. Brimioulle S, Wauthy P, Ewalenko P, et al: Single-beat estimation of right ventricular end-systolic pressure-volume relationship. *Am J Physiol Heart Circ Physiol* 2003; 284:H1625–H1630
42. Trip P, Kind T, van de Veerdonk MC, et al: Accurate assessment of load-independent right ventricular systolic function in patients with pulmonary hypertension. *J Heart Lung Transplant* 2013; 32:50–55
43. Vanderpool RR, Pinsky MR, Naeije R, et al: RV-pulmonary arterial coupling predicts outcome in patients referred for pulmonary hypertension. *Heart* 2015; 101:37–43
44. Vanderpool RR, Puri R, Osorio A, et al: EXPRESS: Surfing the right ventricular pressure waveform: Methods to assess global,

systolic and diastolic RV function from a clinical right heart catheterization. *Pulm Circ* 2019; 10:2045894019850993

45. Haraldsen P, Lindstedt S, Metzsch C, et al: A porcine model for acute ischaemic right ventricular dysfunction. *Interact Cardiovasc Thorac Surg* 2014; 18:43–48
46. Nordhaug D, Steensrud T, Muller S, et al: Intraaortic balloon pumping improves hemodynamics and right ventricular efficiency in acute ischemic right ventricular failure. *Ann Thorac Surg* 2004; 78:1426–1432
47. Calderone A, Jarry S, Couture EJ, et al: Early detection and correction of cerebral desaturation with noninvasive oxy-hemoglobin, deoxy-hemoglobin, and total hemoglobin in cardiac surgery: A case series. *Anesth Analg* 2022; 135:1304–1314
48. Elmi-Sarabi M, Jarry S, Couture EJ, et al: Pulmonary vasodilator response of combined inhaled epoprostenol and inhaled milrinone in cardiac surgical patients. *Anesth Analg* 2022 Sep 15. doi: 10.1213/ane.0000000000006192